A 1D version of EllipSys

van der Laan, Paul; Sørensen, Niels N.

Publication date:
2017

Document Version
Publisher's PDF, also known as Version of record

A 1D version of EllipSys

DTU Wind Energy

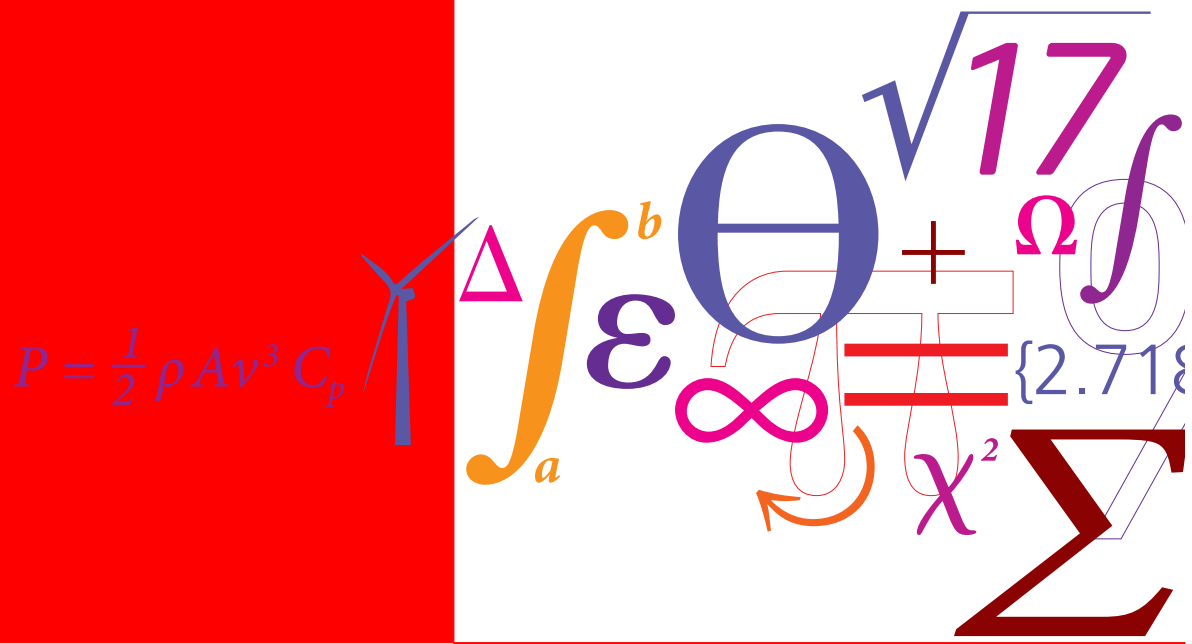

M. Paul van der Laan and Niels N. Sørensen
DTU Wind Energy E-0141
March 2017

DTU Wind Energy
Department of Wind Energy

Contents

1 Introduction

EllipSys is the in-house general purpose flow solver of DTU Wind Energy, developed by Sørensen [10] and Michelsen [8]. Currently, two and thee-dimensional versions exist, referred as EllipSys2D and EllipSys3D, which are suited to perform 2D and 3D Computational Fluid Dynamics (CFD). The main applications of EllipSys are wind turbine rotor aerodynamics and atmospheric flows including terrain, which can be combined to simulate wind turbines operating in realistic flow conditions [12]. It is common to use a precursor simulation to calculate a steady state or transient atmospheric boundary layer (ABL) that can be used as inflow profiles in a CFD simulation. The precursor simulations are currently carried out using EllipSys3D, even though the flow problem is mainly one dimensional. The computational costs of a precursor simulation of a diurnal cycle using EllipSys3D is about 4 hours using 48 cores (198 CPU hours) for simulating 10 days of data. In this report, we introduce a one-dimensional version of EllipSys, referred as EllipSys1D, which can perform precursor simulations much faster while the results compare well with the results from EllipSys3D. For example, a diurnal cycle in EllipSys1D only takes about 10 min using a single core (0.18 CPU hours), which is a reduction of 3 orders of magnitude in CPU hours compared to EllipSys3D. In the atmospheric research community, EllipSys1D could be classified as single-column model. EllipSys1D could also be used for development of new models, since a model implementation in one dimension is often much easier than in two or three dimensions.

The implementation of EllipSys1D is presented in Section 2. A one dimensional grid generation tool is introduced in Section 3. In Section 4, the simulation methodology of three ABL test cases is defined. The test cases are used to compare EllipSys1D with EllipSys3D in Section 5.

2 Implementation

In order for the EllipSys1D code to generate flow that is in discrete balance with the 2D and 3D solvers, and directly allowing implementation of models from 1D to 3D, the code structure is kept nearly identical to the EllipSys2D/3D code. There is only one spatial coordinate in EllipSys1D, which refers to the height z in atmospheric simulations. Therefore, all gradients with respect to x and y can be neglected. The grid is simply a line with distributed cells, which means that all terms related to a curvilinear grid (as used in EllipSys2D and EllipSys3D) can be removed. It is assumed that the advection in z is so small that it can also be neglected, or in other words the velocity in z is zero: $W = 0$. This assumption is valid for neutral steady state atmospheric profiles and an idealized periodic diurnal cycle including effects of temperature. As a result, it is not necessary to solve the W-momentum equation and the pressure correction equation that is normally used to ensure mass conservation. Since EllipSys1D is fast, it is chosen to make the code serial and not use the MPI libraries. In addition, the block structure (basis2D and basis3D[8]) and the multigrid are removed. A full list of features that are removed compared to the EllipSys2/3D code is given below:

- No curvilinear coordinates
- No multigrid
- No block structure (basis2D/basis3D)
- No advection
- No pressure correction solver
- No W-momentum
- No parallelization
- No restart

The coefficient matrix in a 1D finite volume method is tridiagonal. EllipSys1D makes use of this property by solving the coefficient matrix with a tridiagonal solver that solves the matrix very quickly. EllipSys2D and EllipSys3D have more complicated solvers that are slower than the solver implemented in EllipSys1D. This means that one needs to run more iterations in EllipSys2D and

EllipSys3D compared to EllipSys1D in order to reach the same level of convergence.

The current version of EllipSys1D (last changed at 16-01-2017) can run the following auxiliary models:

- keturb: k-ε model[5], k-ε-f_P model[14], k-ε-MO model[15], k-ε-ABL model[4, 9].
- Temperature: temperature equation.
- Output: feature that outputs points of data.

3 Grid generation

The grid in EllipSys1D is a line with distributed cells. The boundary conditions are set at the start and the end of line. The line grid can be generated with a tool called linef90, which is a 1D version of boxf90 that is used to generate Cartesian 3D grids for EllipSys3D. A preprocessor step is not necessary because EllipSys1D does not use the block structure from basis2D and basis3D. An example of an input file for linef90 can be found in Appendix A.1.

4 Methodology

Three test cases based on atmospheric flows are used to compare EllipSys1D with EllipSys3D. The first test case is a logarithmic profile, representing a neutral Atmospheric Surface Layer (ASL). The second test case is a steady state ABL, based on the Leipzig measurements [6]. The last test case represents a periodic diurnal cycle based on the second GEWEX (Global Energy and Water cycle EXperiment) Atmospheric Boundary Layer Study (GABLS2) test case [13].

4.1 Governing equations

An overview of the governing equations that is valid for all test cases is presented here. The Reynolds-averaged Navier-Stokes (RANS) including the Boussinesq approximation [3], and Coriolis and Buoyancy forces can be written as:

$$\underbrace{\frac{DU_i}{Dt}}_{\text{Momentum imbalance}} = \underbrace{-\frac{\partial}{\partial x_j}\left[(\nu+\nu_t)\left(\frac{\partial U_i}{\partial x_j}+\frac{\partial U_j}{\partial x_i}\right)\right]}_{\text{Diffusion}} \underbrace{-\frac{1}{\rho}\frac{\partial \hat{P}}{\partial x_i}}_{\text{Pressure}} \underbrace{+f_c\epsilon_{ijk}e_k\left(U_j-G_j\right)}_{\text{Coriolis}} \underbrace{+g_i(1-\frac{\rho_0}{\rho})}_{\text{Buoyancy}} \tag{1}$$

Here we assume that z is the vertical coordinate, and x and y are horizontal coordinates. In addition, U_i are the velocity components, x_j are spatial coordinates, ν is the molecular viscosity, ν_T is the turbulent eddy viscosity, $\hat{P} = P - \frac{2}{3}\rho k$ is the modified pressure with P as the pressure, ρ as the density and k as the turbulent kinetic energy. The Coriolis term is balanced by prescribed geostrophic wind G_i, where f_c is the Coriolis parameter that depends on the latitude, ϵ_{ijk} is the Levi-Civita symbol and e_k is the normal vector in the z direction. In the buoyancy term, $g_i = \{0, 0, g\}^T$ is the gravitational acceleration vector with g as the gravitational acceleration constant and ρ_0 is the reference density.

The turbulence is modeled by a modified version of the k-ε model of Launder and Spalding [5]. The turbulent eddy viscosity ν_T is defined as:

$$\nu_T = C_\mu \frac{k^2}{\varepsilon}, \tag{2}$$

with ε as the turbulent dissipation and C_μ as a constant. The turbulent quantities k and ε are determined from transport equations:

$$\frac{Dk}{Dt} = \frac{\partial}{\partial x_j}\left[\left(\nu + \frac{\nu_T}{\sigma_k}\right)\frac{\partial k}{\partial x_j}\right] + \mathcal{P} - (\varepsilon - \varepsilon_{\text{amb}}) + B, \tag{3}$$

$$\frac{D\varepsilon}{Dt} = \frac{\partial}{\partial x_j}\left[\left(\nu + \frac{\nu_T}{\sigma_\epsilon}\right)\frac{\partial \varepsilon}{\partial x_j}\right] + \left(C^*_{\varepsilon,1}\mathcal{P} - C_{\varepsilon,2}\varepsilon + C_{\varepsilon,3}B\right)\frac{\varepsilon}{k} + C_{\varepsilon,2}\frac{\varepsilon^2_{\text{amb}}}{k_{\text{amb}}}, \tag{4}$$

where $\mathcal{P}$ is the turbulent production due to shear, B is turbulent production or destruction due to buoyancy, k_{amb} and ε_{amb} are ambient value of k and ε, and $C^*_{\varepsilon,1}, C_{\varepsilon,2}$, $C_{\varepsilon,3}$ σ_k, σ_ε are constants or relations. $C^*_{\epsilon 1}$ is defined as:

$$C^*_{\epsilon 1} = C_{\epsilon 1} + (C_{\epsilon 2} - C_{\epsilon 1})\frac{\ell_t}{\ell_{t,\max}}, \tag{5}$$

and it is used to limit the ABL height as introduced by Apsley and Castro [1]. ℓ_t is the turbulent length scale and $\ell_{t,\max}$ is the maximum allowed turbulent length scale. In neutral conditions (Leipzig test case), $\ell_{t,\max}$ is constant and it is determined from the relation of Blackadar $\ell_{t,\max} = 0.00027G/|f_c|$, with G as the magnitude of the geostrophic wind vector G_i.

When effects of temperature are modeled, as performed in the GABLS2 test case, the buoyancy is modeled as:

$$B = -\frac{\nu_T}{\sigma_\theta}\frac{g}{\theta}\frac{\partial \theta}{\partial z}, \tag{6}$$

where θ is the potential temperature that is modeled by a transport equation:

$$\frac{D\theta}{Dt} = \frac{\partial}{\partial x_j}\left[\left(\mu + \frac{\mu_t}{\sigma_\theta}\right)\frac{\partial \theta}{\partial x_j}\right] + S_\theta\ , \tag{7}$$

where S_θ are heat sources and σ_θ is a model constant or a relation. In the GABLS2 test case, the potential temperature is relaxed towards the initial temperature profile over a time span of one day to enforce diurnal periodicity. The initial profile is a constant (289 K) up to 4000 m and then increases with 3.5 K per 1 km.

The following buoyancy related parameterizations for σ_θ and $C_{\epsilon 3}$ are used:

$$\sigma_\theta = \begin{cases} 0.74 & Ri_G > 0 \\ 0.74\,(1 - 15Ri_G)^{-1/4} & Ri_G < 0 \end{cases}, \text{with } Ri_G = -B/\left(\mathcal{P} + \left|\frac{\alpha_\beta}{\sigma_\theta}B\right|\right) \tag{8}$$

$$C_{\epsilon,3} = (C_{\epsilon,1} - C_{\epsilon,2})\alpha_B + 1, \tag{9}$$

where α_B is defined as:

$$\alpha_B = \begin{cases} 1 - \frac{\ell}{\ell_{t,\max}} & \text{if} \quad Ri_g > 0 \\ 1 - [1 + \frac{C_{\epsilon,2}-1}{C_{\epsilon,2}-C_{\epsilon,1}}]\frac{\ell}{\ell_{t,\max}} & \text{if} \quad Ri_g < 0 \end{cases} \text{ with } Ri_g = -B/\mathcal{P} \tag{10}$$

In addition, $\ell_{t,\max}$ is parametrized by an integration of the ABL as introduced by Mellor and Yamada[7]:

$$\ell_{t,\max} = 0.075\frac{\int_0^\infty z\sqrt{k}dz}{\int_0^\infty \sqrt{k}dz} \tag{11}$$

The density is related to the potential temperature using the ideal gas law:

$$\rho = \frac{MP_0}{R\theta}, \tag{12}$$

where $M = 29$ g/mol is the average molar mass of air, $P_0 = 10^5$ Pa is the standard atmospheric pressure, and $R = 8.313$ J/mol/K is the universal gas constant.

The turbulence model constants and input parameters are listed in Tables 1 and 2, respectively. Note that u_* represents the friction velocity.

Table 1: Model constants.

Case	C_μ	$C_{\varepsilon,1}$	$C_{\varepsilon,2}$	$C_{\varepsilon,3}$	σ_k	σ_ε	κ	σ_θ
ASL	0.03	1.21	1.92	0	1.00	1.30	0.40	-
Leipzig	0.03	1.21	1.92	0	1.00	1.30	0.40	-
GABLS2	0.03	1.52	1.833	eq.9	2.95	2.95	0.40	eq. 8

Table 2: Input parameters.

Case	u_* [m/s]	z_0 [m]	G [m/s]	$\ell_{t,\max}$ [m]	f_c [1/s]	g [m/s^2]	k_{amb} [m^2/s^2]	ε_{amb} [m^2/s^3]
ASL	0.4	0.05	-	∞	0	0	0	0
Leipzig	-	0.3	17.5	41.8	1.13×10^{-4}	0	10^{-4}	7.208×10^{-8}
GABLS2	-	0.03	9.5	eq. 11	8.87×10^{-5}	9.81	10^{-4}	7.208×10^{-8}

4.2 Grid and boundary conditions

The 1D and 3D Cartesian grids are shown in Figure 1. The grid is 6 km tall and the 3D grid is 40 m wide in horizontal dimensions, x and y. 192 cells are used in the normal (z) direction, using a first cell height of 0.1 m. 4 cells with uniform spacing of 10 m is applied in the horizontal dimensions of the 3D grid, resulting in 48 blocks of 4^3 cells.

A wall boundary condition (BC) is applied at $z = z_0$, where z_0 is the roughness length, which is consistent with a neutral ASL profile [11]. In the ASL test case, an inlet BC is applied at $z = 6$ km where the analytical solution is set, while a symmetric BC is used both in the Leipzig and GABLS2 test cases. The remaining side boundaries of the 3D grid are set to periodic BCs. In the

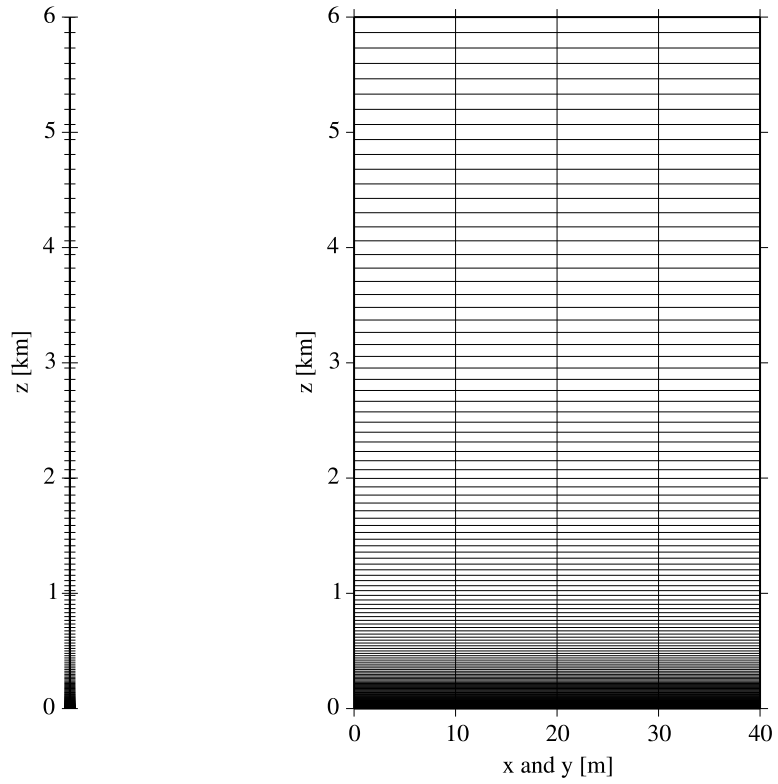

Figure 1: Grid for the 1D (left) and 3D (right) simulations.

GABLS2 test case, a time varying temperature is prescribed at the wall BC that reflects a diurnal variation in temperature.

The input files of the 1D and 3D grids are given in Appendices A.1 and A.2.

5 Results and Discussion

The results of the three ABL test cases are presented in three following sections. The EllipSys1D and EllipSys3D input files are given in Appendices A.3, A.4, A.5, A.6, A.7 and A.8.

5.1 ASL

In both the 1D and 3D simulations, the flow domain is initialized by the analytical solution of the ASL:

$$U(z) = \frac{u_*}{\kappa} \ln\left(\frac{z}{z_0}\right), \qquad k = \frac{u_*^2}{\sqrt{C_\mu}}, \qquad \varepsilon(z) = \frac{u_*^3}{\kappa z}, \qquad \nu_T = u_* \kappa z \tag{13}$$

In the 1D simulation, the profiles of U, k and ε do not change up the 10th digit after 60000 iterations. In the 3D simulation, a convergence in order of 10^{-6} is achieved after 820000 iterations. This shows that the current numerical setup is quite inefficient for EllipSys3D. The final profiles are plotted in Figure 2 and compared with the analytical solution of eq. 13. The k profile and velocity profile (to a lesser extent) differ from the analytical solution because of the well known wall problem [2]. The simulated profiles compare very well with each other. The normalized difference between the 1D and 3D solution, defined as:

$$\Delta\phi = (\phi_{1D} - \phi_{3D})/\phi_{3D}, \tag{14}$$

is plotted in Figure 3. Note that ϕ_{1D} and ϕ_{3D} represent results of a flow variable of the 1D and 3D versions of EllipSys, respectively. Figure 3 shows that the difference between EllipSys1D and EllipSys3D results is in the order of the convergence level of the EllipSys3D simulation.

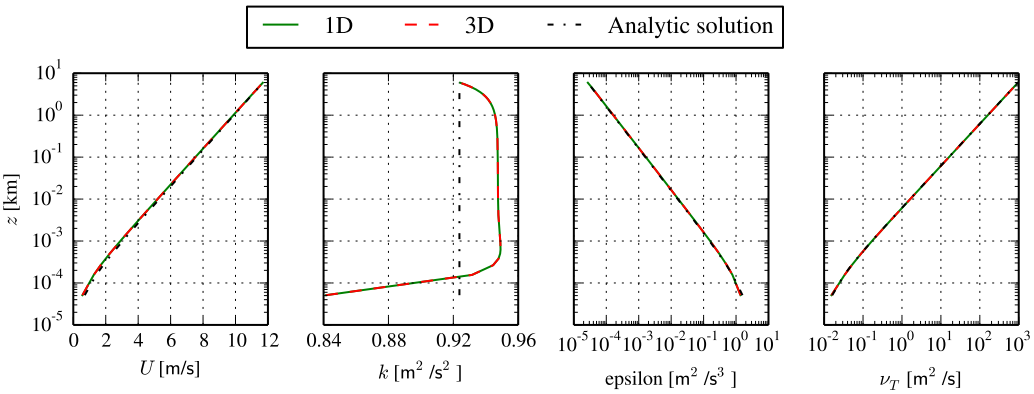

Figure 2: 1D and 3D results of the logarithmic surface layer test case.

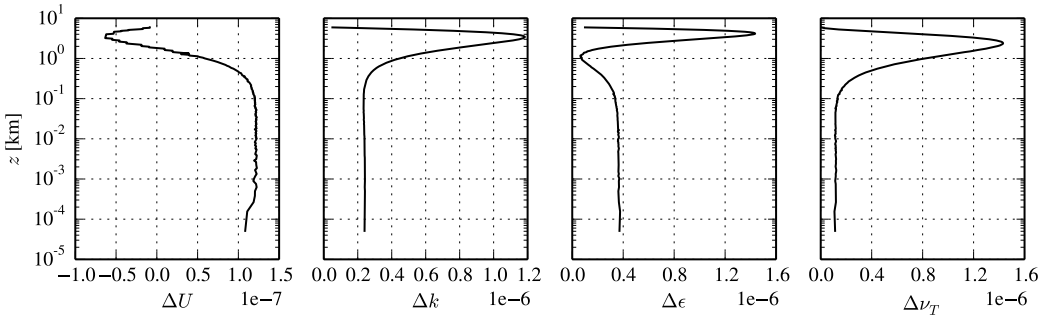

Figure 3: Normalized difference between 1D and 3D results of the logarithmic surface layer test case.

5.2 Leipzig profile

Although the flow problem of the Leipzig test case is steady state, it is solved in transient mode using a fixed time step of 100 s and 8 subiterations to avoid numerical problems in the 1D solver. When the Leipzig test case is run in steady state using the 1D solver, the flow solution diverges. The 3D solver can be used in steady state mode without numerical problems. This indicates that the 1D solver behaves more stiff compared to the 3D solver.

The 1D and 3D results of the Leipzig profiles are shown in Figure 4. A solution after 10^4 and 10^5 iterations are plotted for both simulations. The 1D simulation is converged after 10^4 iteration while the 3D simulations needs 10^5 iterations to compare well with the 1D simulation.

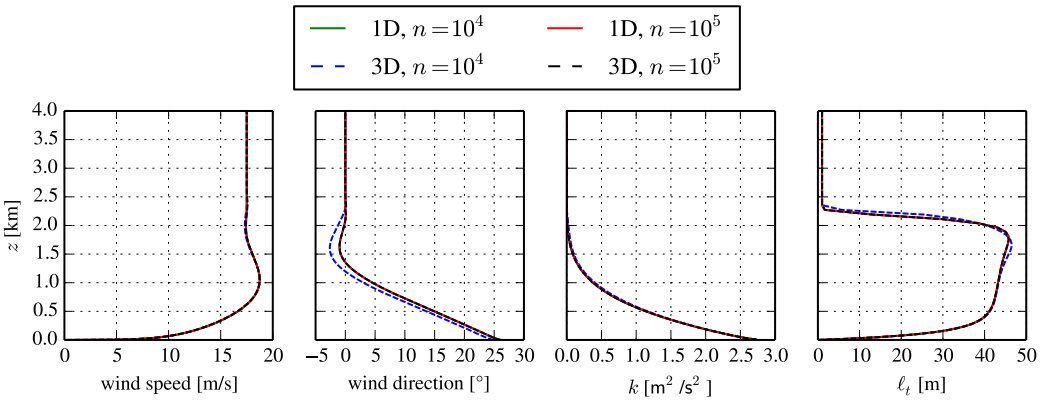

Figure 4: 1D and 3D results of the Leipzig test case, as function of number of iterations.

Figure 5 shows the normalized difference as defined in eq. (14) between the 1D and 3D simulations for a different number of iterations of the 3D simulation: 10^4, 10^5 and 10^6. Note the error in wind direction is normalized by $\max(\phi_{3D}) - \min(\phi_{3D})$ to avoid a devision by zero. The largest error occur around the ABL height. It is clear that the difference between the 1D and 3D simulations becomes smaller for longer run times. We can conclude the both EllipSys1D and EllipSys3D calculates the same solution of the Leipzig test case, as long as the number of iterations is large enough.

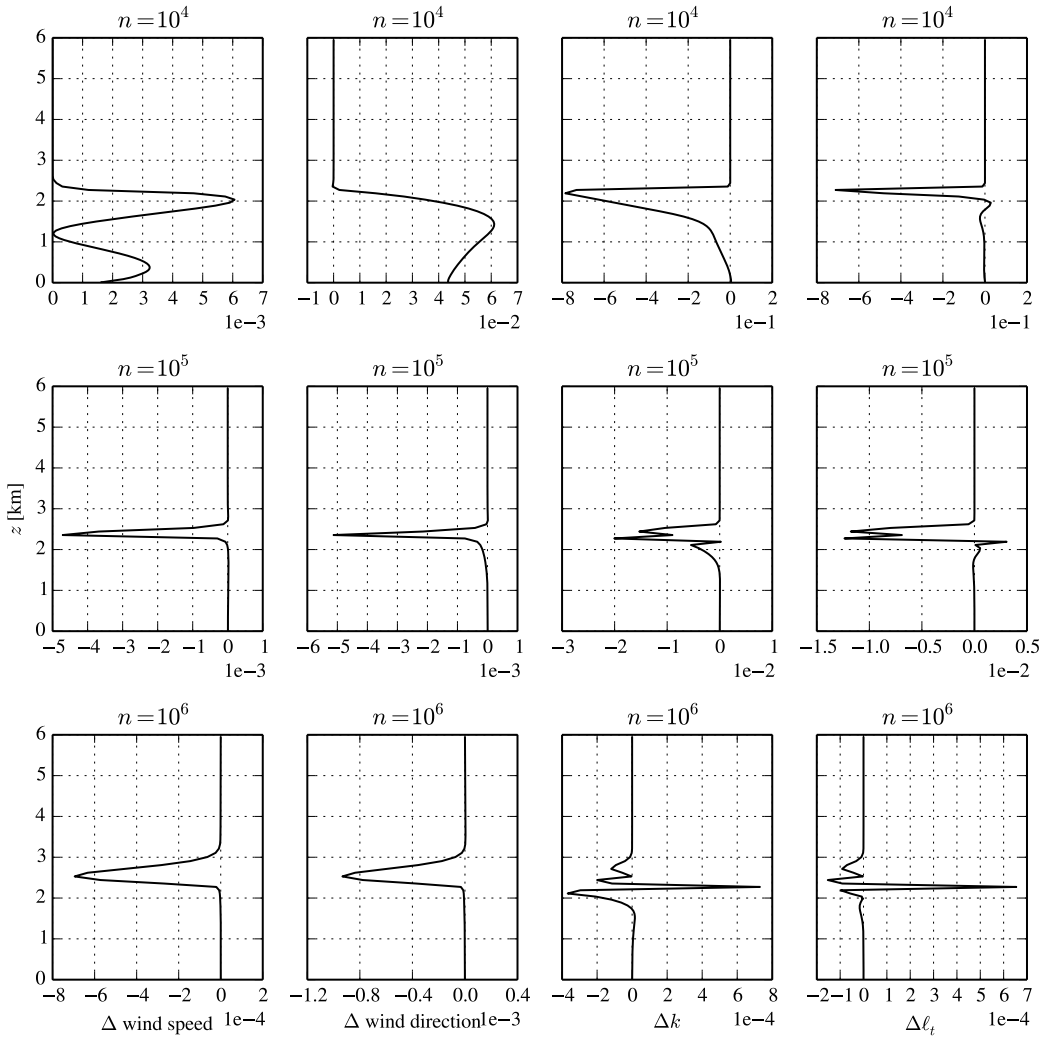

Figure 5: Normalized difference between 1D and 3D results of the Leipzig test case, as function of number of iterations.

5.3 GABLS2

The GABLS2 test case is simulated for 10 days using a time step of 1 s and 8 subiterations. The results of the last day is used to compare the 1D and 3D simulations. Contours of wind speed, wind direction, k and potential temperature are plotted as function of height and time in Figure 6 for both solvers. In the bottom plots, the wall temperature is shown as a black line. The normalized differences, as defined in eq. (14), between the 1D and 3D simulations are plotted in the right column of Figure 6. Since k can become close to zero, it is normalized by $\max(\phi_{3D}) - \min(\phi_{3D})$. Overall, the differences between the 1D and 3D simulations are small. The largest differences are observed around the ABL height, especially at the time of the day where the wall heats up quickly. This is also visible in Figure 7, where 4 profiles are plotted at different times of the day for both the 1D and 3D simulations. There are only small visible differences mainly occurring near the ABL height for all shown times and also below the ABL height at 12:00 h when the change in wall temperature is relatively large.

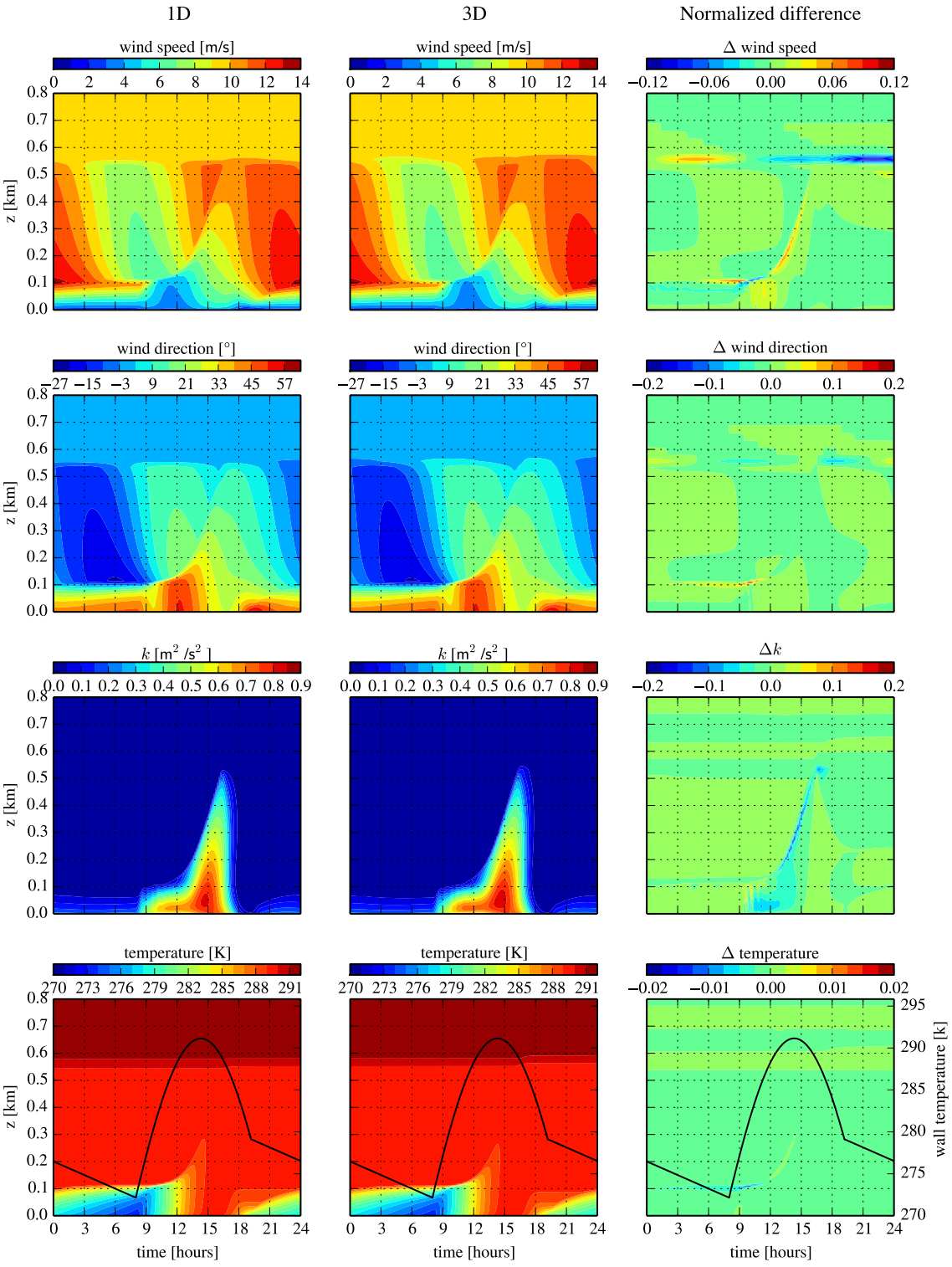

Figure 6: 1D (left column) and 3D (middle column) results and normalized difference (right column) of the GABLS2 test case. Wall temperature is shown as a black line in bottom plots.

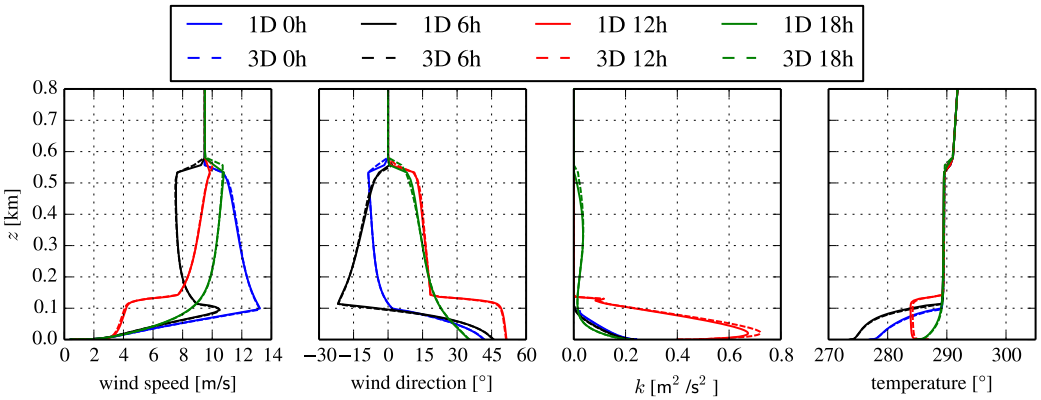

Figure 7: 1D and 3D results of the GABLS2 test case.

5.4 Computational costs

The Leipzig and GABLS2 test cases represent typical precursor simulations that can be used as inlet conditions in a larger CFD simulation of flow over terrain (including wind turbines). It is often necessary to perform parametric runs of precursor simulations in order to obtain the desired inflow conditions. Therefore, it is interesting to compare the computational costs of the EllipSys1D and EllipSys3D for the Leipzig and the GABLS3 test cases, as listed in Table 3. The EllipSys1D simulation of the Leipzig test case takes 6 s on a single core (0.0017 CPU hours), while the EllipSys3D simulation takes 20 min using 48 cores (16 CPU hours). Hence, EllipSys1D is about 10^4 faster than EllipSys3D to obtain a converged solution. The 3D simulation of the GABLS2 test case takes 4 hours and 8 minutes wall clock time using 48 cores (198 CPU hours), while the 1D simulation only takes 10 minutes and 53 seconds to complete on a single core (0.18 CPU hours), which is reduction of 3 order of magnitude in terms of CPU hours.

Table 3: Computational cost of EllipSys1D and EllipSys3D to obtain a converged solution of the Leipzig and GABLS2 test cases.

	EllipSys1D		EllipSys3D		ratio CPU hours
Case	wall clock time	CPU hours	wall clock time	CPU hours	EllipSys3D/EllipSys1D
Leipzig	6 s	0.0017	20 min	16	9400
GABLS2	10 min 53 s	0.18	4 h 08 min	198	1100

All simulations are carried out on the Jess computer cluster, consisting of Intel Xeon E5-2680v2 processors that have 10 cores running at 2.8 GHz.

6 Conclusion

A one-dimensional version of EllipSys, labeled as EllipSys1D is presented. Three atmospheric boundary layer test cases are used to show that results of EllipSys1D are exactly the same or very similar as results of EllipSys3D, while EllipSys1D uses 3 to 4 orders of magnitude less CPU hours compared to EllipSys3D.

References

[1] D. D. Apsley and I. P. Castro. A limited-length-scale k-ε model for the neutral and stably-stratified atmospheric boundary layer. Boundary-Layer Meteorology, 83:75–98, 1997.

[2] B. Blocken, T. Stathopoulos, and J. Carmeliet. CFD simulation of the atmospheric boundary layer: wall function problems. Atmospheric Environment, 41:238–252, 2007.

[3] M. J. Boussinesq. Théorie de l'écoulement tourbillonnant et tumultueux des liquides. Gauthier-Villars et fils, Paris, France, 1897.

[4] T. Koblitz, A. Bechmann, A. Sogachev, N. Sørensen, and P.-E. Réthoré. Computational fluid dynamics model of stratified atmospheric boundary-layer flow. Wind Energy, 18:75–89, 2015.

[5] B. E. Launder and D. B. Spalding. Mathematical models of turbulence. Academic Press, London, UK, 1972.

[6] H. Lettau. A re-examination of the Leipzig wind profile considering some relations between wind and turbulence in the frictional layer. Tellus, 2(2):125–129, 1950.

[7] G. L. Mellor and T. Yamada. A hierarchy of turbulence closure models for planetary boundary layers. Journal of the Atmospheric Sciences, 31:1791–1806, 1974.

[8] J. A. Michelsen. Basis3d - a platform for development of multiblock PDE solvers. Technical Report AFM 92-05, Technical University of Denmark, Lyngby, Denmark, 1992.

[9] A. Sogachev, M. Kelly, and M. Y. Leclerc. Consistent two-equation closure modelling for atmospheric research: Buoyancy and vegetation implementations. Boundary-Layer Meteorology, 145:307–327, 2012.

[10] N. N. Sørensen. General purpose flow solver applied to flow over hills. PhD thesis, Risø National Laboratory, Roskilde, Denmark, 1994.

[11] N. N. Sørensen, A. Bechmann, J. Johansen, L. Myllerup, P. Botha, S. Vinther, and B. S. Nielsen. Identification of severe wind conditions using a Reynolds Averaged Navier-Stokes solver. Journal of Physics: Conference series, 75(012053):1–13, 2007.

[12] N. N. Sørensen, J. C. Heinz, M. P. van der Laan, P. E. Réthoré, N. Troldborg, and F. Zahle. The Problem of Multiple Scales in CFD Simulations of Wind Turbine Aerodynamics. In International Conference on Model Integration across Disparate Scales in Complex Turbulent Flow Simulation - State College, PA, United States, 2015.

[13] G. Svensson, A. A. M. Holtslag, V. Kumar, T. Mauritsen, G. J. Steeneveld, E. Angevine, W. M.and Bazile, A. Beljaars, E. I. F. de Bruijn, A. Cheng, L. Conangla, J. Cuxart, M. Ek, M. J. Falk, F. Freedman, H. Kitagawa, V. E. Larson, Lock. A., J. Mailhot, V. Masson, S. Park, J. Pleim, S. Söderberg, W. Weng, and M. Zampieri. Evaluation of the diurnal cycle in the atmospheric boundary layer over land as represented by a variety of single-column models: The second GABLS experiment. 140:177–206, 2011.

[14] M. P. van der Laan, N. N. Sørensen, P.-E. Réthoré, J. Mann, M. C. Kelly, N. Troldborg, J. G. Schepers, and E. Machefaux. An improved k-ε model applied to a wind turbine wake in atmospheric turbulence. Wind Energy, 18(5):889–907, May 2015. doi: 10.1002/we.1736.

[15] M. P. van der Laan, N. N. Sørensen, and M. C. Kelly. A new k-epsilon model consistent with Monin-Obukhov similarity theory. Wind Energy, 20(3):479–489, 2017. doi: 10.1002/we.2017.

A Input files

A.1 1D grid

ASL:

```
ni 193
len 6000
bc 101 201
distribution 2 0 0.00001666666666667 1 1 -1 193
```

Leipzig/GABLS2:

```
ni 193
len 6000
bc 101 601
distribution 2 0 0.00001666666666667 1 1 -1 193
```

A.2 3D grid

ASL:

```
ni 5
nj 5
nk 193
xlen 40
ylen 40
zlen 6000
xbc 501 501
ybc 502 502
zbc 101 201
x-distribution 2 0 0.25 1 1 0.25 5
y-distribution 2 0 0.25 1 1 0.25 5
z-distribution 2 0 0.00001666666666667 1 1 -1 193
```

Leipzig/GABLS2:

```
ni 5
nj 5
nk 193
xlen 40
ylen 40
zlen 6000
xbc 501 501
ybc 502 502
zbc 101 601
x-distribution 2 0 0.25 1 1 0.25 5
y-distribution 2 0 0.25 1 1 0.25 5
z-distribution 2 0 0.00001666666666667 1 1 -1 193
```

A.3 EllipSys1D ASL

```
project grid
mstep 1000000
reslim 1.d-6
density 1.225d0
viscosity 1.78406d-5
vinlet 0.d0
vfarfield 0.d0
field v value 0d0
relaxu 0.7
uinlet 0.4
ufarfield 10.0
field u value 10.0
func-const z0 0.05
func-const uStar 0.4
func-const kappa 0.4
func-const cmu 0.03
inlet u 201 300 value uStar/kappa*log((z+z0)/z0)
inlet v 201 300 value 0.0
inlet w 201 300 value 0.0
inlet tke 201 300 value uStar**2/sqrt(cmu)
inlet dtke 201 300 value uStar**3/(kappa*(z+z0))
field u value uStar/kappa*log((z+z0)/z0)
field v value 0.0
field w value 0.0
field tke value uStar**2/sqrt(cmu)
field dtke value uStar**3/(kappa*(z+z0))
turbulence kepsilon
ke_version rough
loglaw true
ce1 1.20941505331
ce2 1.92
prtke_ke 1.0
pred_ke 1.3
cmu 0.03
relaxturb 0.7
roughness 0.05
te_inlet 1.00d0
ed_inlet 0.001d0
te_farfield 1.00d0
ed_farfield 0.001d0
output true
nroutput 10000
extract_var tke
extract_var dtke
extract_var vis
extract-line-zcc
```

A.4 EllipSys1D Leipzig

```
project grid
mstep 100000
reslim 1.d-8
```

```
relaxu .6d0
subiterations 8
transient true 100.d0
density 1.225d0
viscosity 1.78406d-5
uinlet 0.d0
vinlet 0.d0
func-const teamb 1.d-4
func-const edamd 7.208434d-8
field w value 0.0
field tke value teamb
field dtke value edamd
turbulence kepsilon
ke_version rough-abl
loglaw true
cmu 0.03
ce1 1.20941505330508
ce2 1.92
pred_ke 1.3
prtke_ke 1.0
relaxturb 0.6
te_inlet 1.0d-1
ed_inlet 0.003d0
ufarfield 12.374368671
vfarfield 12.374368671
field u value 12.374368671
field v value 12.374368671
roughness 0.3d0
turb_cori true 0.000113
lmax 41.8d0
ambient_ke 1d-4 7.208434d-8
output true
nroutput 1000
extract_var tke
extract_var dtke
extract_var vis
extract-line-zcc
```

A.5 EllipSys1D GABSL2

```
project grid
mstep 864000
subiterations 8
reslim 1.d-4
transient true 1.d0
relaxu .7d0
density 1.225d0
viscosity 1.78406d-5
ufarfield 6.717514421
vfarfield 6.717514421
func-const teini 0.1
func-const edini 0.003d0
field u value 6.717514421
field v value 6.717514421
```

```
field w value 0.0
field tke value teini
field dtke value edini
gravitation -9.81
temperature air
prandtl 0.74 0.74
prandtl_var
inlet temp 100 151 file 1 Twalllow.dat
field temp value 289+(z+0.1)*3.5d-3
field temp min 289+(4000+0.1)*3.5d-3
temp_inlet 289
temp_wall 289
temp_relaxation
temp_farfield 289
relaxtemp 0.6
turbulence kepsilon
ke_version rough-abl
loglaw true
roughness 0.03
lmaxmy 0.075
ambient_ke 1.0d-4 7.208d-8
kappa 0.4
cmu 0.03
ce1 1.52
ce2 1.833
pred_ke 2.95131
prtke_ke 2.95131
relaxturb 6.0d-1
te_inlet 1.0d-1
ed_inlet 0.003d0
te_farfield 1.0d-1
ed_farfield 0.003d0
turb_cori true 8.87d-5
output true
nroutput 600
extract_var temperature
extract_var tke
extract_var dtke
extract_var lmax
extract_var uf
extract_var heatflux
extract_var prandtltempvar
extract_var den
extract-line-zcc
```

A.6 EllipSys3D ASL

```
project grid
grid_level 1
mstep 1000000
reslim 1.d-6 1.d-5
reslimp 2.d-1
diff_scheme quick
pres_corr simple
```

```
interpolationorder 2
nrgraphout 100
nrrestart 100000
relaxp 0.2d0
density 1.225d0
viscosity 1.78406d-5
vinlet 0.d0
vfarfield 0.d0
field v value 0d0
winlet 0.d0
wfarfield 0.d0
field w value 0d0
relaxu 0.7
uinlet 0.4
ufarfield 10.0
field u value 10.0
func-const z0 0.05
func-const uStar 0.4
func-const kappa 0.4
func-const cmu 0.03
inlet u 201 300 value uStar/kappa*log((z+z0)/z0)
inlet v 201 300 value 0.0
inlet w 201 300 value 0.0
inlet tke 201 300 value uStar**2/sqrt(cmu)
inlet dtke 201 300 value uStar**3/(kappa*(z+z0))
field u value uStar/kappa*log((z+z0)/z0)
field v value 0.0
field w value 0.0
field tke value uStar**2/sqrt(cmu)
field dtke value uStar**3/(kappa*(z+z0))
turbulence kepsilon
ke_version rough
loglaw true
ce1 1.20941505331
ce2 1.92
prtke_ke 1.0
pred_ke 1.3
cmu 0.03
relaxturb 0.7
roughness 0.05
te_inlet 1.00d0
ed_inlet 0.001d0
te_farfield 1.00d0
ed_farfield 0.001d0
output true
nroutput 10000
extract_var tke
extract_var dtke
extract-point 20.00000000 20.00000000 0.05113467 0.05113467
extract-point 20.00000000 20.00000000 0.15574225 0.15574225
extract-point 20.00000000 20.00000000 0.26513318 0.26513318
extract-point 20.00000000 20.00000000 0.37952610 0.37952610
extract-point 20.00000000 20.00000000 0.49914962 0.49914962
extract-point 20.00000000 20.00000000 0.62424281 0.62424281
extract-point 20.00000000 20.00000000 0.75505567 0.75505567
extract-point 20.00000000 20.00000000 0.89184953 0.89184953
```

```
extract-point 20.00000000 20.00000000 1.03489770 1.03489770
extract-point 20.00000000 20.00000000 1.18448600 1.18448600
extract-point 20.00000000 20.00000000 1.34091334 1.34091334
extract-point 20.00000000 20.00000000 1.50449213 1.50449213
extract-point 20.00000000 20.00000000 1.67554905 1.67554905
extract-point 20.00000000 20.00000000 1.85442587 1.85442587
extract-point 20.00000000 20.00000000 2.04147970 2.04147970
extract-point 20.00000000 20.00000000 2.23708412 2.23708412
extract-point 20.00000000 20.00000000 2.44162985 2.44162985
extract-point 20.00000000 20.00000000 2.65552497 2.65552497
extract-point 20.00000000 20.00000000 2.87919664 2.87919664
extract-point 20.00000000 20.00000000 3.11309131 3.11309131
extract-point 20.00000000 20.00000000 3.35767582 3.35767582
extract-point 20.00000000 20.00000000 3.61343843 3.61343843
extract-point 20.00000000 20.00000000 3.88088912 3.88088912
extract-point 20.00000000 20.00000000 4.16056167 4.16056167
extract-point 20.00000000 20.00000000 4.45301419 4.45301419
extract-point 20.00000000 20.00000000 4.75882957 4.75882957
extract-point 20.00000000 20.00000000 5.07861765 5.07861765
extract-point 20.00000000 20.00000000 5.41301679 5.41301679
extract-point 20.00000000 20.00000000 5.76269316 5.76269316
extract-point 20.00000000 20.00000000 6.12834325 6.12834325
extract-point 20.00000000 20.00000000 6.51069683 6.51069683
extract-point 20.00000000 20.00000000 6.91051520 6.91051520
extract-point 20.00000000 20.00000000 7.32859427 7.32859427
extract-point 20.00000000 20.00000000 7.76576796 7.76576796
extract-point 20.00000000 20.00000000 8.22290617 8.22290617
extract-point 20.00000000 20.00000000 8.70091836 8.70091836
extract-point 20.00000000 20.00000000 9.20075732 9.20075732
extract-point 20.00000000 20.00000000 9.72341697 9.72341697
extract-point 20.00000000 20.00000000 10.26993633 10.26993633
extract-point 20.00000000 20.00000000 10.84140307 10.84140307
extract-point 20.00000000 20.00000000 11.43895432 11.43895432
extract-point 20.00000000 20.00000000 12.06377699 12.06377699
extract-point 20.00000000 20.00000000 12.71711176 12.71711176
extract-point 20.00000000 20.00000000 13.40025835 13.40025835
extract-point 20.00000000 20.00000000 14.11457236 14.11457236
extract-point 20.00000000 20.00000000 14.86147075 14.86147075
extract-point 20.00000000 20.00000000 15.64243779 15.64243779
extract-point 20.00000000 20.00000000 16.45902150 16.45902150
extract-point 20.00000000 20.00000000 17.31283982 17.31283982
extract-point 20.00000000 20.00000000 18.20558746 18.20558746
extract-point 20.00000000 20.00000000 19.13903037 19.13903037
extract-point 20.00000000 20.00000000 20.11501840 20.11501840
extract-point 20.00000000 20.00000000 21.13548607 21.13548607
extract-point 20.00000000 20.00000000 22.20244627 22.20244627
extract-point 20.00000000 20.00000000 23.31801164 23.31801164
extract-point 20.00000000 20.00000000 24.48438988 24.48438988
extract-point 20.00000000 20.00000000 25.70387787 25.70387787
extract-point 20.00000000 20.00000000 26.97888611 26.97888611
extract-point 20.00000000 20.00000000 28.31193329 28.31193329
extract-point 20.00000000 20.00000000 29.70563951 29.70563951
extract-point 20.00000000 20.00000000 31.16275423 31.16275423
extract-point 20.00000000 20.00000000 32.68614990 32.68614990
extract-point 20.00000000 20.00000000 34.27881429 34.27881429
extract-point 20.00000000 20.00000000 35.94388225 35.94388225
```

```
extract-point 20.00000000 20.00000000 37.68462842 37.68462842
extract-point 20.00000000 20.00000000 39.50445838 39.50445838
extract-point 20.00000000 20.00000000 41.40694484 41.40694484
extract-point 20.00000000 20.00000000 43.39581928 43.39581928
extract-point 20.00000000 20.00000000 45.47496166 45.47496166
extract-point 20.00000000 20.00000000 47.64844170 47.64844170
extract-point 20.00000000 20.00000000 49.92050920 49.92050920
extract-point 20.00000000 20.00000000 52.29558218 52.29558218
extract-point 20.00000000 20.00000000 54.77829390 54.77829390
extract-point 20.00000000 20.00000000 57.37348159 57.37348159
extract-point 20.00000000 20.00000000 60.08617281 60.08617281
extract-point 20.00000000 20.00000000 62.92163893 62.92163893
extract-point 20.00000000 20.00000000 65.88538209 65.88538209
extract-point 20.00000000 20.00000000 68.98311937 68.98311937
extract-point 20.00000000 20.00000000 72.22084366 72.22084366
extract-point 20.00000000 20.00000000 75.60479843 75.60479843
extract-point 20.00000000 20.00000000 79.14149973 79.14149973
extract-point 20.00000000 20.00000000 82.83775494 82.83775494
extract-point 20.00000000 20.00000000 86.70063353 86.70063353
extract-point 20.00000000 20.00000000 90.73754245 90.73754245
extract-point 20.00000000 20.00000000 94.95620666 94.95620666
extract-point 20.00000000 20.00000000 99.36464545 99.36464545
extract-point 20.00000000 20.00000000 103.97125803 103.97125803
extract-point 20.00000000 20.00000000 108.78480077 108.78480077
extract-point 20.00000000 20.00000000 113.81435966 113.81435966
extract-point 20.00000000 20.00000000 119.06944737 119.06944737
extract-point 20.00000000 20.00000000 124.55997662 124.55997662
extract-point 20.00000000 20.00000000 130.29622805 130.29622805
extract-point 20.00000000 20.00000000 136.28896019 136.28896019
extract-point 20.00000000 20.00000000 142.54937821 142.54937821
extract-point 20.00000000 20.00000000 149.08909643 149.08909643
extract-point 20.00000000 20.00000000 155.92026266 155.92026266
extract-point 20.00000000 20.00000000 163.05552154 163.05552154
extract-point 20.00000000 20.00000000 170.50797067 170.50797067
extract-point 20.00000000 20.00000000 178.29127776 178.29127776
extract-point 20.00000000 20.00000000 186.41973054 186.41973054
extract-point 20.00000000 20.00000000 194.90806897 194.90806897
extract-point 20.00000000 20.00000000 203.77161724 203.77161724
extract-point 20.00000000 20.00000000 213.02645493 213.02645493
extract-point 20.00000000 20.00000000 222.68913122 222.68913122
extract-point 20.00000000 20.00000000 232.77683634 232.77683634
extract-point 20.00000000 20.00000000 243.30759422 243.30759422
extract-point 20.00000000 20.00000000 254.29993479 254.29993479
extract-point 20.00000000 20.00000000 265.77308665 265.77308665
extract-point 20.00000000 20.00000000 277.74719329 277.74719329
extract-point 20.00000000 20.00000000 290.24293752 290.24293752
extract-point 20.00000000 20.00000000 303.28175727 303.28175727
extract-point 20.00000000 20.00000000 316.88608793 316.88608793
extract-point 20.00000000 20.00000000 331.07893175 331.07893175
extract-point 20.00000000 20.00000000 345.88409912 345.88409912
extract-point 20.00000000 20.00000000 361.32647933 361.32647933
extract-point 20.00000000 20.00000000 377.43154714 377.43154714
extract-point 20.00000000 20.00000000 394.22563162 394.22563162
extract-point 20.00000000 20.00000000 411.73621807 411.73621807
extract-point 20.00000000 20.00000000 429.99138251 429.99138251
extract-point 20.00000000 20.00000000 449.02009058 449.02009058
```

```
extract-point 20.00000000 20.00000000 468.85253309 468.85253309
extract-point 20.00000000 20.00000000 489.51947827 489.51947827
extract-point 20.00000000 20.00000000 511.05260303 511.05260303
extract-point 20.00000000 20.00000000 533.48486474 533.48486474
extract-point 20.00000000 20.00000000 556.84975985 556.84975985
extract-point 20.00000000 20.00000000 581.18168981 581.18168981
extract-point 20.00000000 20.00000000 606.51637164 606.51637164
extract-point 20.00000000 20.00000000 632.88999027 632.88999027
extract-point 20.00000000 20.00000000 660.33960139 660.33960139
extract-point 20.00000000 20.00000000 688.90358343 688.90358343
extract-point 20.00000000 20.00000000 718.62066962 718.62066962
extract-point 20.00000000 20.00000000 749.53039007 749.53039007
extract-point 20.00000000 20.00000000 781.67356783 781.67356783
extract-point 20.00000000 20.00000000 815.09121540 815.09121540
extract-point 20.00000000 20.00000000 849.82501857 849.82501857
extract-point 20.00000000 20.00000000 885.91787907 885.91787907
extract-point 20.00000000 20.00000000 923.41265958 923.41265958
extract-point 20.00000000 20.00000000 962.35271170 962.35271170
extract-point 20.00000000 20.00000000 1002.78246817 1002.78246817
extract-point 20.00000000 20.00000000 1044.74601953 1044.74601953
extract-point 20.00000000 20.00000000 1088.28768923 1088.28768923
extract-point 20.00000000 20.00000000 1133.45267864 1133.45267864
extract-point 20.00000000 20.00000000 1180.28545840 1180.28545840
extract-point 20.00000000 20.00000000 1228.83039427 1228.83039427
extract-point 20.00000000 20.00000000 1279.13244893 1279.13244893
extract-point 20.00000000 20.00000000 1331.23537159 1331.23537159
extract-point 20.00000000 20.00000000 1385.18237928 1385.18237928
extract-point 20.00000000 20.00000000 1441.01692041 1441.01692041
extract-point 20.00000000 20.00000000 1498.78064781 1498.78064781
extract-point 20.00000000 20.00000000 1558.51416162 1558.51416162
extract-point 20.00000000 20.00000000 1620.25784121 1620.25784121
extract-point 20.00000000 20.00000000 1684.04958936 1684.04958936
extract-point 20.00000000 20.00000000 1749.92564501 1749.92564501
extract-point 20.00000000 20.00000000 1817.92149229 1817.92149229
extract-point 20.00000000 20.00000000 1888.06936736 1888.06936736
extract-point 20.00000000 20.00000000 1960.39915191 1960.39915191
extract-point 20.00000000 20.00000000 2034.93937066 2034.93937066
extract-point 20.00000000 20.00000000 2111.71445756 2111.71445756
extract-point 20.00000000 20.00000000 2190.74574391 2190.74574391
extract-point 20.00000000 20.00000000 2272.05208037 2272.05208037
extract-point 20.00000000 20.00000000 2355.64877875 2355.64877875
extract-point 20.00000000 20.00000000 2441.54632037 2441.54632037
extract-point 20.00000000 20.00000000 2529.75105829 2529.75105829
extract-point 20.00000000 20.00000000 2620.26648179 2620.26648179
extract-point 20.00000000 20.00000000 2713.08994517 2713.08994517
extract-point 20.00000000 20.00000000 2808.21394822 2808.21394822
extract-point 20.00000000 20.00000000 2905.62754693 2905.62754693
extract-point 20.00000000 20.00000000 3005.31288000 3005.31288000
extract-point 20.00000000 20.00000000 3107.24661034 3107.24661034
extract-point 20.00000000 20.00000000 3211.40150250 3211.40150250
extract-point 20.00000000 20.00000000 3317.74277362 3317.74277362
extract-point 20.00000000 20.00000000 3426.22971725 3426.22971725
extract-point 20.00000000 20.00000000 3536.81746607 3536.81746607
extract-point 20.00000000 20.00000000 3649.45319904 3649.45319904
extract-point 20.00000000 20.00000000 3764.07796496 3764.07796496
extract-point 20.00000000 20.00000000 3880.62864453 3880.62864453
```

```
extract-point 20.00000000 20.00000000 3999.03404738 3999.03404738
extract-point 20.00000000 20.00000000 4119.21694609 4119.21694609
extract-point 20.00000000 20.00000000 4241.09624320 4241.09624320
extract-point 20.00000000 20.00000000 4364.58299113 4364.58299113
extract-point 20.00000000 20.00000000 4489.58263698 4489.58263698
extract-point 20.00000000 20.00000000 4615.99738874 4615.99738874
extract-point 20.00000000 20.00000000 4743.72218718 4743.72218718
extract-point 20.00000000 20.00000000 4872.64714854 4872.64714854
extract-point 20.00000000 20.00000000 5002.66011081 5002.66011081
extract-point 20.00000000 20.00000000 5133.64258002 5133.64258002
extract-point 20.00000000 20.00000000 5265.47234362 5265.47234362
extract-point 20.00000000 20.00000000 5398.02616320 5398.02616320
extract-point 20.00000000 20.00000000 5531.17571021 5531.17571021
extract-point 20.00000000 20.00000000 5664.79030864 5664.79030864
extract-point 20.00000000 20.00000000 5798.73972767 5798.73972767
extract-point 20.00000000 20.00000000 5932.89088265 5932.89088265
```

A.7 EllipSys3D Leipzig

```
project grid
grid_level 1
mstep 1000000
mstepp 5
subiterations 8
reslim 1.d-6
reslimp 2.d-1
diff_scheme quick
pres_corr simplea 1.0 1.0
pres_levels 5
interpolationorder 2
nrrestart 1000000
transient true 100.d0
relaxu .7d0
relaxp .2d0
density 1.225d0
viscosity 1.78406d-5
winlet 0.d0
uinlet 0.4d0
wfarfield 0.d0
turbulence kepsilon
ke_version rough-abl
turbcrossterms false
loglaw true
ambient_ke 1.0d-4 7.208d-8
cmu 0.03
ce1 1.20941505330508
ce2 1.92
pred_ke 1.3
prtke_ke 1.0
relaxturb 6.0d-1
te_inlet 1.0d-1
ed_inlet 0.003d0
te_farfield 1.0d-1
ed_farfield 0.003d0
```

```
forceallocation
ufarfield 12.374368671
field u value 12.374368671
vfarfield 12.374368671
field v value 12.374368671
roughness 0.3d0
turb_cori true 0.000113
lmax 41.8
ambient_ke 1d-4 7.208434d-8
output true
nroutput 1000
extract_var tke
extract_var dtke
extract_var lmax
```

+ the extraxt-point lines as defined in the input file of Section A.6.

A.8 EllipSys3D GABSL2

```
project grid
grid_level 1
mstep 864000
mstepp 5
subiterations 8
reslim 1.d-4
reslimp 2.d-1
diff_scheme quick
pres_corr simplea 1.0 1.0
pres_levels 5
interpolationorder 2
nrrestart 1000000
transient true 1.d0
relaxu .7d0
relaxp .2d0
density 1.225d0
viscosity 1.78406d-5
winlet 0.d0
uinlet 0.4d0
wfarfield 0.d0
ufarfield 6.717514421
vfarfield 6.717514421
gravitation 0 0 -9.81
temperature air
prandtl 0.74 0.74
prandtl_var
inlet temp 100 151 file 1 Twalllow.dat
field temp value 289+(z+0.1)*3.5d-3
field temp min 289+(4000+0.1)*3.5d-3
temp_inlet 289
temp_wall 289
temp_relaxation
temp_farfield 289
relaxtemp 0.6
turbulence kepsilon
ke_version rough-abl
```

```
turbcrossterms false
loglaw true
roughness 0.03
lmaxmy 0.075
ambient_ke 1.0d-4 7.208d-8
cmu 0.03
ce1 1.52
ce2 1.833
pred_ke 2.95131
prtke_ke 2.95131
relaxturb6.0d-1
te_inlet 1.0d-1
ed_inlet 0.003d0
te_farfield 1.0d-1
ed_farfield 0.003d0
forceallocation
turb_cori true 8.87d-5
output true
nroutput 600
extract_var temperature
extract_var tke
extract_var dtke
extract_var lmax
extract_var uf
extract_var heatflux
extract_var prandtltempvar
```

+ the extraxt-point lines as defined in the input file of Section A.6.

DTU Wind Energy
Department of Wind Energy
Technical University of Denmark

Risø Campus Building 118
Frederiksborgvej 399
DK-4000 Roskilde
www.vindenergi.dtu.dk

DTU Wind Energy E-0141
ISBN: 978-87-93549-08-1